



Cite this: *Org. Biomol. Chem.*, 2025, **23**, 5215

Synthesis of 6-arylpyrimido[4,5-e]indolizine-2,4(1H,3H)-diones through InCl_3 -catalyzed cycloisomerization†

Ruben Manuel Figueira de Abreu, Alexander Villinger, Peter Ehlers and Peter Langer *

We report the synthesis of hitherto unknown pyrimido[4,5-e]indolizine-2,4(1H,3H)-diones (indolizinouracils) and related polycondensed uracils. The synthetic strategy is based on a chemoselective C–N coupling through an addition–elimination reaction of *N,N*-dimethyl-5-bromo-6-chlorouracil with N-heterocycles, followed by Sonogashira cross-coupling reaction with alkynes and InCl_3 -catalysed cycloisomerisation. The methodology allows for the employment of pyrrole and indole as N-heterocyclic building blocks and tolerates various functional groups. The impact of the substitution pattern on the photophysical properties was studied by steady-state UV-Vis and fluorescence spectroscopy, providing new insights into the potential applications of uracil-based polycondensed heterocycles.

Received 11th March 2025,
Accepted 24th April 2025

DOI: 10.1039/d5ob00436e
rsc.li/obc

Introduction

Pyrimidines and related compounds, such as uracils (pyrimidine-2,4-diones), play key roles in cellular processes and, hence, have evolved as valuable building blocks in modern drug development. They are key components of nucleosides; they form the highly ordered double helix structures of DNA and RNA and hence are fundamental for coding genetic information and ensuring proper functioning of living cells.^{1,2} Apart from their presence in DNA and RNA, pyrimidines are also found in a variety of natural products, such as xanthines, pteridines, pyrrolopyrimidines and pyridopyrimidines. They possess various biological activities such as anti-bacterial, anti-proliferative, antifungal and anti-inflammatory activities.^{3–5} Hence, there has been considerable interest in the synthesis and properties of fused pyrimidine derivatives, which has led to the discovery of several synthetic drugs, such as pemetrexed (A), immucilin H (B), ganciclovir (C) and ruxolitinib (D) (Fig. 1).^{1,6}

Traditionally, fused pyrimidines are obtained using two different approaches. The first synthetic methodology utilizes pre-functionalized heterocycles, and the pyrimidine ring is constructed by employing suitable urea derivatives. The

second approach takes advantage of the reactivity of pyrimidine derivatives, and a fused heterocyclic entity is directly constructed on the pyrimidine scaffold.⁷ Our group has contributed to the latter strategy by employing easily available uracil derivatives followed by sequential functionalisation through substitution and Pd-catalysed cross-coupling reactions.^{8,9}

As an extension of our ongoing interest in the synthesis of heterocyclic fused uracils, we herein report the synthesis of indolizinouracils. While pyrrolo- and pyridouracils are well known and represent intriguing building blocks in medicinal chemistry,^{1,4,5,10} indolizinouracils have, to the best of our knowledge, not been previously reported in the literature.¹¹ Our synthetic approach is based on a three-step procedure, involving a chemoselective reaction of 6-chloro-5-bromouracil with N-heterocycles, such as pyrrole and indole, followed by a Sonogashira reaction¹² and subsequent cycloisomerisation (Scheme 1).

Results and discussion

Synthesis

5-Bromo-6-chlorouracil (**1**) was prepared as reported in the literature.^{8,13} Starting material **1** was further functionalized by nucleophilic substitution with pyrrole as the corresponding heteroaromatic nucleus. Initially, NaH was chosen as a base as it allows complete deprotonation of pyrrole. However, TLC monitoring revealed poor conversion of uracil **1**, even after prolonged reaction time. Hence, we next employed *n*-BuLi at -78°C as the base. Using this base at lower temperature fol-

Universität Rostock, Institut für Chemie, Albert-Einstein-Str. 3a, 18059 Rostock, Germany. E-mail: peter.langer@uni-rostock; Fax: +49 381 498 6412; Tel: +49 381 498 6410

† Electronic supplementary information (ESI) available. CCDC 2428779. For ESI and crystallographic data in CIF or other electronic format see DOI: <https://doi.org/10.1039/d5ob00436e>



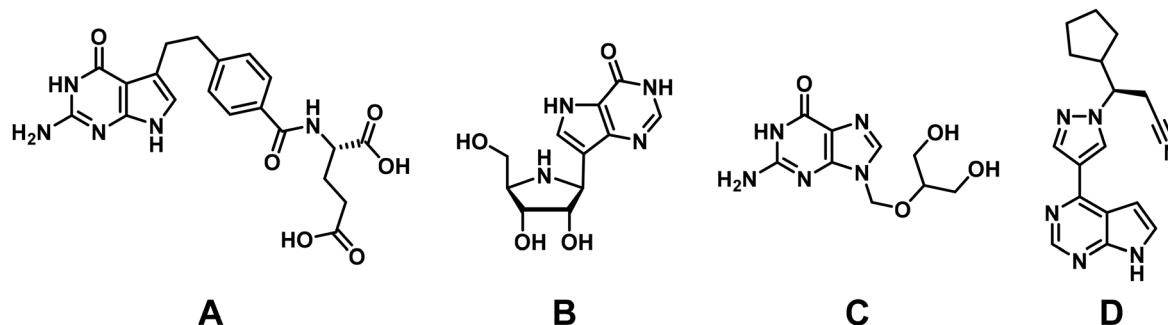
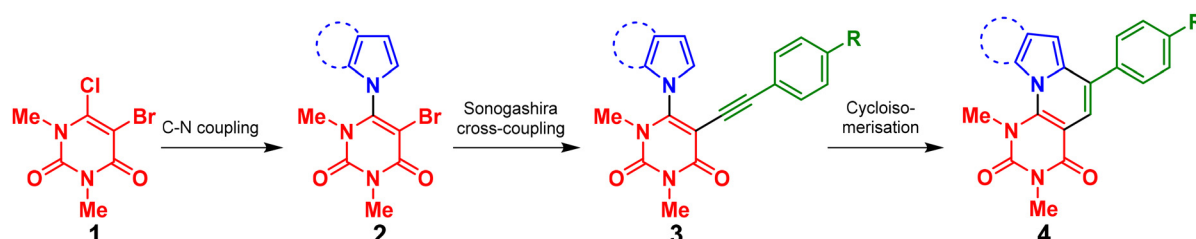


Fig. 1 Chemical structures of pemetrexed (A), immucilin H (B), ganciclovir (C) and ruxolitinib (D).

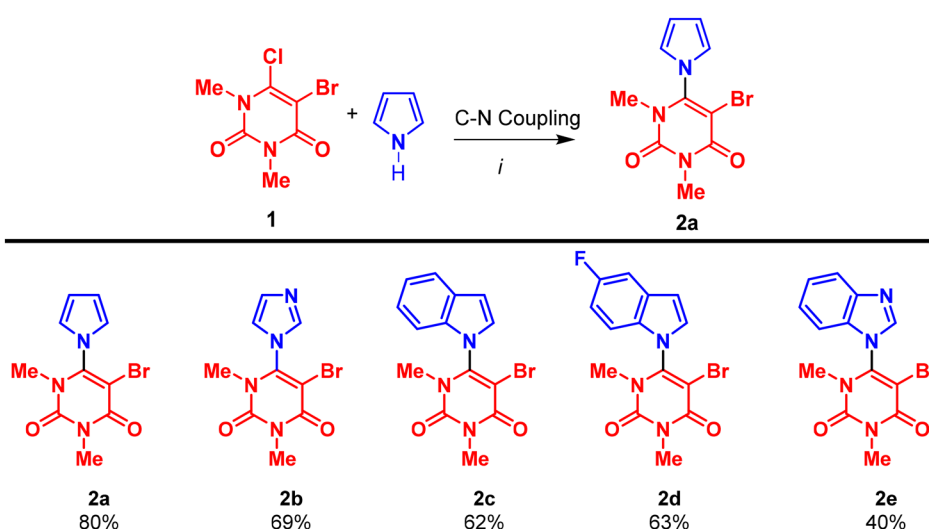


Scheme 1 Synthetic strategy.

lowed by slow warming to room temperature gave the corresponding pyrrole-substituted uracil **2a** in 80% yield (Scheme 2). The developed reaction conditions were also applicable to other N-heterocycles, such as imidazole, indole and benzimidazole and gave the corresponding products in good yields. Only the reaction with benzimidazole delivered the corresponding product in only a moderate isolated yield of 40%, which was due to difficulties encountered during its purification by column chromatography.

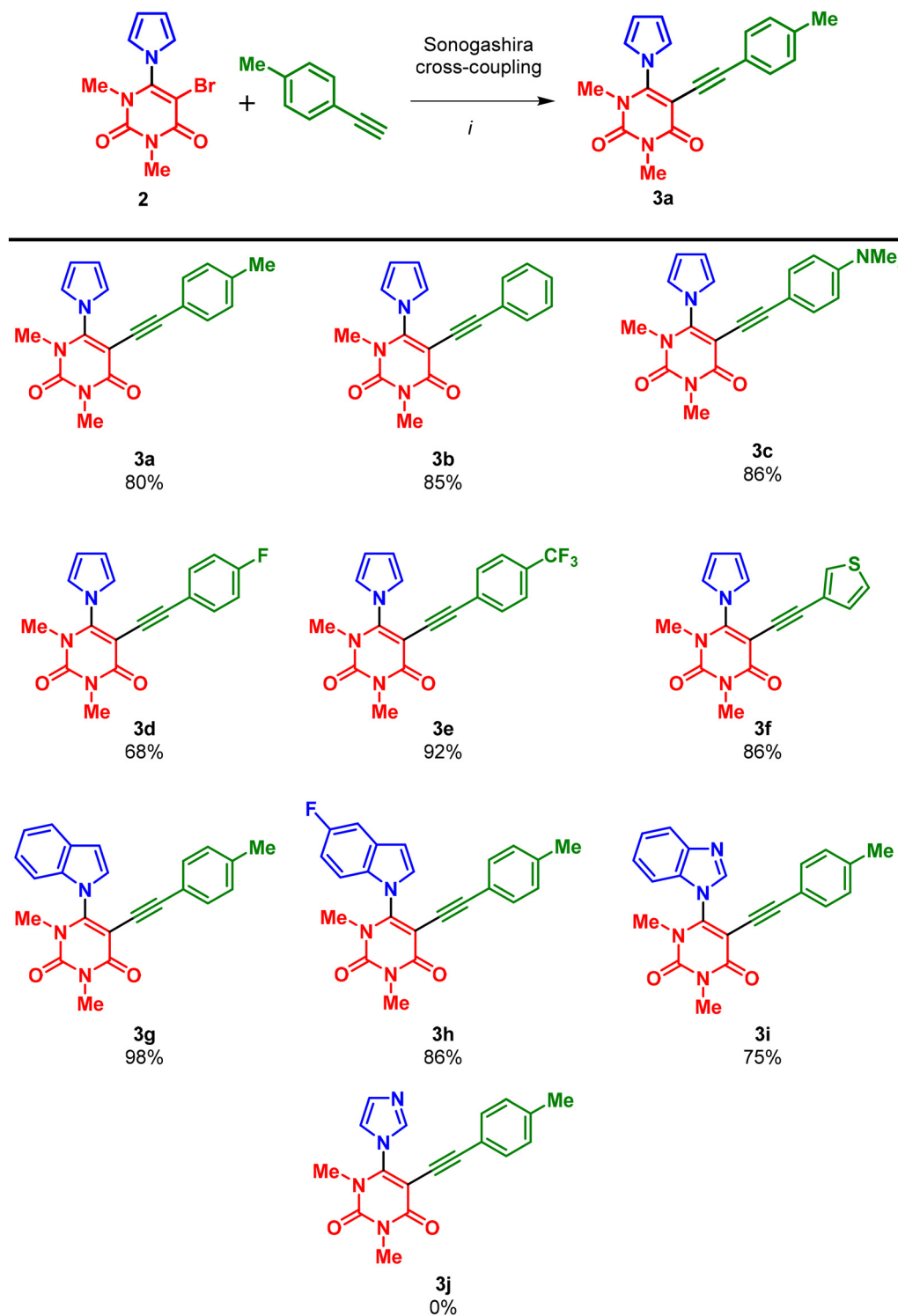
Subsequently, the Sonogashira reaction of **2a** with 4-tolylacetylene was studied. As an initial attempt, our previously

developed conditions for the Sonogashira reaction of alkynes with uracil derivatives were employed.⁸ Using $\text{Pd}(\text{PPh}_3)_4$ in the presence of CuI as the co-catalyst and triethylamine as the base in DMSO led to the desired coupling product **3a** in 80% yield. Hence, no further optimisation of the reaction conditions was required, and the scope of the reaction was studied next. The reaction of **2a** and **c–e**, containing pyrrole, indole and benzimidazole substituents, with various arylacetylenes afforded products **3a–i** (Scheme 3). Products **3a–i** were isolated in good to very good yields, ranging from 68–98%. The obtained yields were independent of both the substitution



Scheme 2 Synthesis of uracils **2a–e**. Reaction conditions: (i) $n\text{-BuLi}$, azol, THF, $-78\text{ }^\circ\text{C} \rightarrow 24\text{ }^\circ\text{C}$, 7 h. Yields of isolated products.



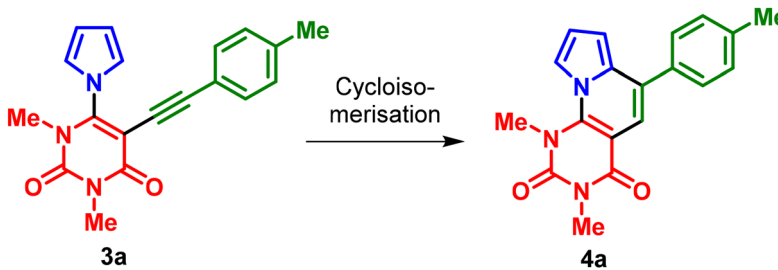


Scheme 3 Synthesis of **3a–i**. Reaction conditions: arylacetylene (1.2 equiv.), $\text{Pd}(\text{PPh}_3)_4\text{Cl}_2$ (5 mol%), CuI (5 mol%), NEt_3 (11 equiv.), DMSO, 100 °C, 6 h. Yields of isolated products.

pattern of the employed aryl acetylene and the nature of the heterocycle attached to the uracil ring. Employment of the imidazole-substituted uracil **2b** failed to give product **3j**. Despite complete conversion of the starting material, we were

not able to purify the product from other impurities (which were also not detectable by TLC analysis).

Finally, we studied the cycloisomerisation of **3a** as a model substrate to access the desired indolizinouracil **4a** (Table 1). As

Table 1 Optimization of the synthesis of **4a**


Entry	Acid (equiv.)	Solvent	Temperature (°C)	Time (h)	Yield (%)
1	<i>p</i> -TsOH·H ₂ O (15)	Toluene	100	6	31
2	<i>p</i> -TsOH·H ₂ O (20)	Toluene	100	6 (16)	30
3	MsOH (20)	Toluene	100	6 (16)	11
4	TFA (20)	Toluene	100	6 (16)	37
5	PtCl ₂ (0.1)	Toluene	80	6 (16)	Mixture
6	PtCl ₂ (0.1)	Toluene	100	6 (16)	Mixture
7	InCl ₃ (0.05)	Toluene	80	6 (16)	29
8	InCl ₃ (0.1)	Toluene	100	16	76
9	InCl ₃ (1)	Toluene	100	16	72

As a starting point of our investigation, we used *p*-TsOH·H₂O as the Brønsted acid, given its good performance in previously reported transformations.⁹ Using this acid in toluene at 100 °C gave the desired product, albeit in only 31% yield. Subsequently, we screened different Brønsted acids, such as methanesulfonic acid (MsOH) and trifluoroacetic acid (TFA). Unfortunately, the yields could not be significantly increased. Consequently, we turned our attention to Lewis acids. In the beginning, PtCl₂ was employed, which is known to efficiently catalyse the cycloisomerisation of 2-biaryl alkynes due to its π -electron affinity.^{14,15} However, only complex mixtures, which could not be purified, were obtained. However, employment of catalytic amounts of InCl₃ (10 mol%) eventually gave **4a** in 76% isolated yield.^{14,16} Increasing the amount of InCl₃ to an equimolar ratio resulted in no further improvement.

With the optimised conditions in hand, InCl₃ (0.1 equiv.), toluene, 100 °C, 16 h, the scope of the cycloisomerisation reaction was investigated. The cycloisomerization of **3a–h** worked very well and products **4a–h** were mostly obtained in good to very good yields (Scheme 4). Only compound **4c**, containing a strongly electron-donating NMe₂ group, was obtained in a moderate 46% yield. This can be explained by problems during the purification caused by the low solubility of **4c**. In the case of benzimidazole-substituted uracil **3i**, no conversion was observed and, hence, product **4i** could not be obtained, possibly due to the coordination of InCl₃ or the formation of imidazolyl cations under acidic conditions.

The highest yield of 86% was obtained for the fluorine-substituted compound **4d**. In general, the reaction conditions do not seem to be affected by the substitution pattern of the arylalkyne moiety, as all compounds (except **4c**) were obtained in similar yields.

The structure was unambiguously verified by analysis of the spectroscopic data. The characteristic carbon signals of the

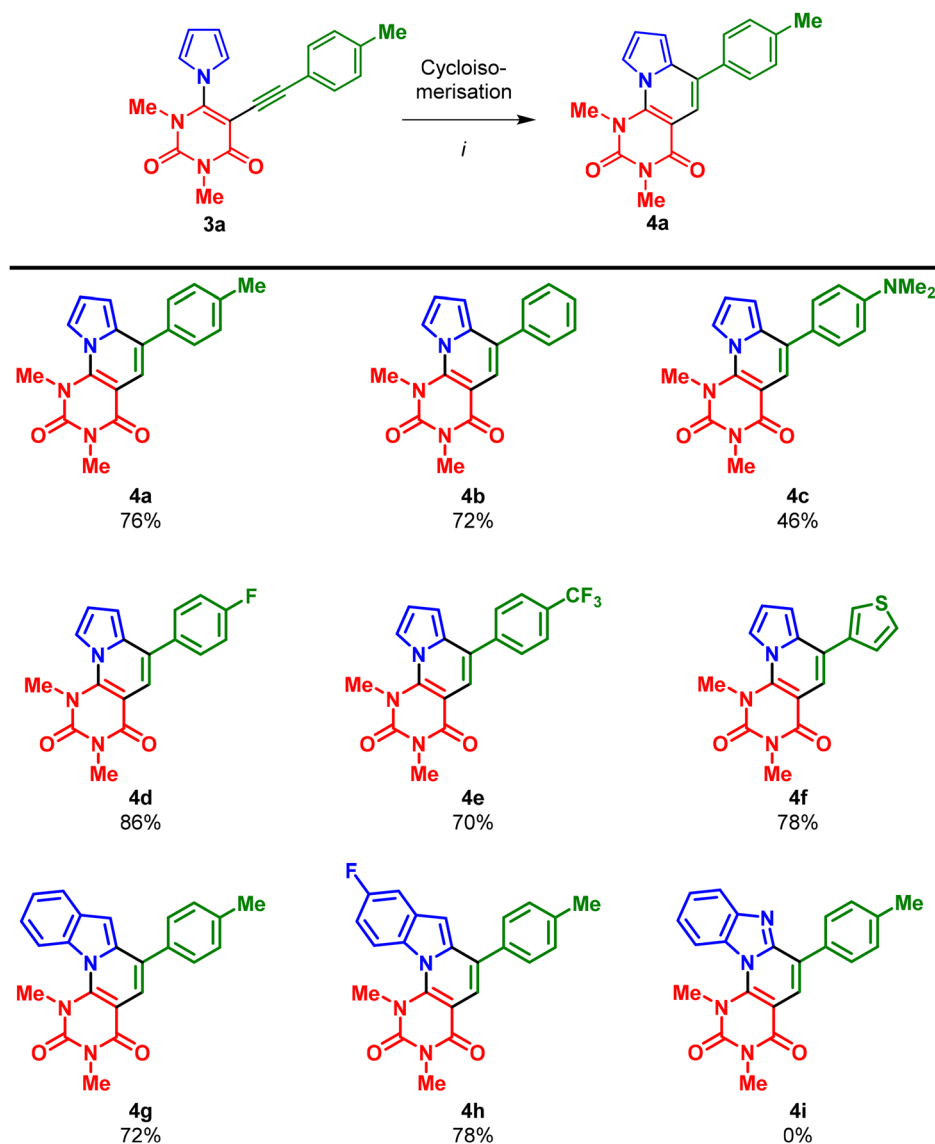
triple bond disappeared and a typical vinylic proton signal was observed. Moreover, the loss of symmetry in the pyrrole ring indicated its functionalisation while mass spectroscopy revealed the same molar mass but with different fragmentation. Moreover, the structure of **4a** was independently confirmed by X-ray crystallographic analysis. Crystals were obtained by slow evaporation from a mixture of dichloromethane and heptane at room temperature (Fig. 2). Product **4a** crystallises in a base-centred monoclinic system with the *P2₁/n* space group. The analysis revealed the formation of a planar indolizinouracil core structure. The substituted tolyl ring is twisted out of plane by 47°. Two molecules align in a parallel, slipped head-to-tail orientation with several short CH- π (2.76 Å) and CC- π contacts (3.39 Å), while neighbouring molecules form hydrogen bonds between the carbonyl oxygen and the hydrogen of the adjacent methyl (2.32 Å) and pyrrole ring.

Optical properties

The photophysical properties of selected derivatives were investigated by steady-state absorption and photoluminescence spectroscopy. The influence of the substitution pattern of arylated indolizinouracils on the photophysical properties is shown in Fig. 3. Corresponding photophysical data and quantum yields are given in Table 2.

Compounds **4b**, **4e** and **4f** show very similar absorption and emission properties. All three compounds possess their lowest absorption band ($S_0 \rightarrow S_1$) at approximately 375 nm with comparable extinction coefficients (3700–4600 M⁻¹ cm⁻¹) and emission maxima at ~470 nm. Interestingly, **4c** containing a strongly electron-donating NMe₂-group shows a slight bathochromic shift of its absorption features accompanied by enhanced extinction coefficients. In contrast, the emission maximum of **4c** is hypsochromically shifted to 419 nm. Moreover, while all measured compounds show low quantum





Scheme 4 Synthesis of 4a–h. Reaction conditions: InCl_3 (0.1 equiv.), toluene, $100\text{ }^\circ\text{C}$, 16 h. Yields of isolated products.

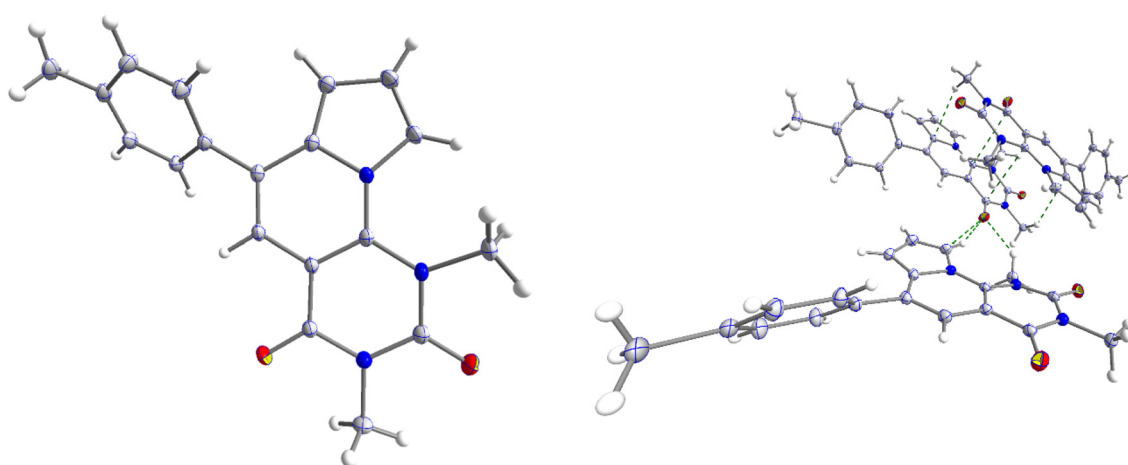


Fig. 2 ORTEP of 4a (left); short contact interactions within the crystal lattice (right). Element colours: carbon (grey), hydrogen (white), oxygen (red) and nitrogen (blue). The thermal ellipsoids are drawn at the 50% probability level.



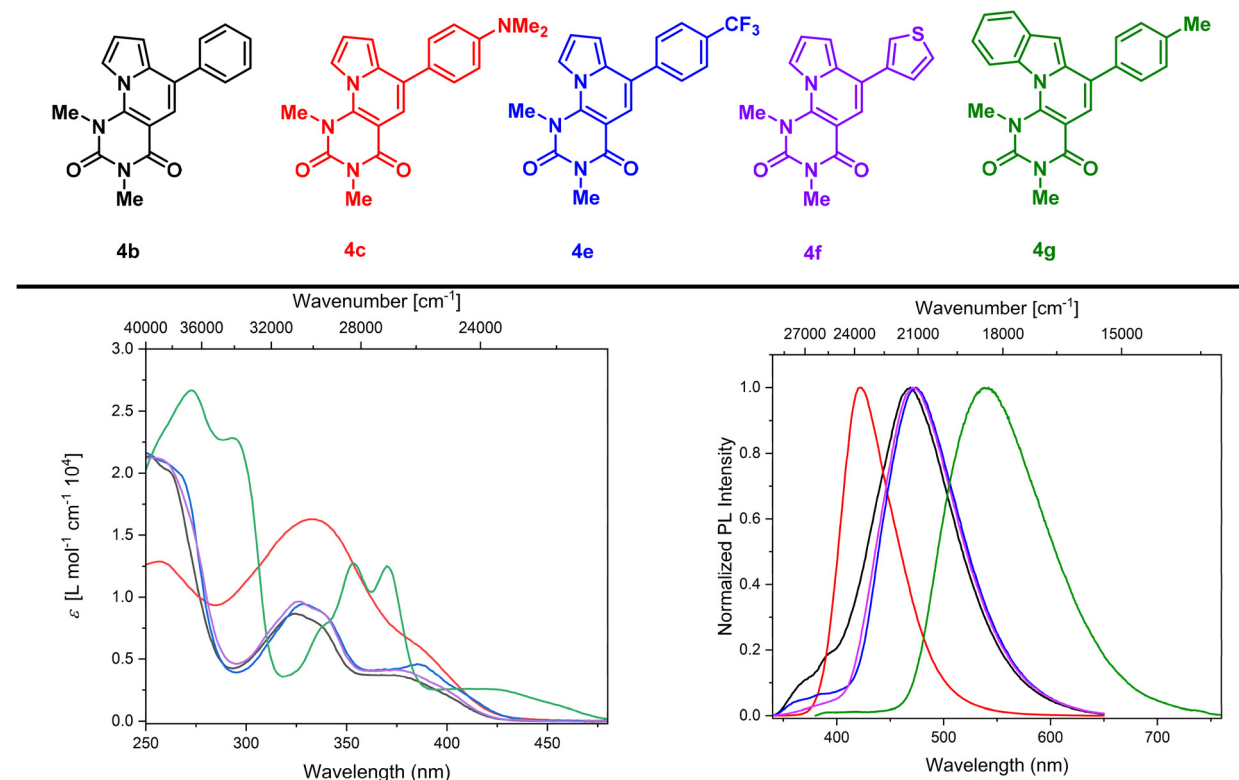


Fig. 3 UV-vis absorption (left) and emission (right, $\lambda_{\text{ex}} = 330$ nm and $\lambda_{\text{ex}} = 370$ nm (**4g**)) spectra of 1,3-dimethyl-6-(aryl)pyrimido[4,5-e]indolizine-2,4(1H,3H)-dione derivatives (**4b**, **4c**, **4e**, **4f**, and **4g**) in dichloromethane ($c = 1 \times 10^{-5}$ M).

Table 2 Photophysical data of selected 1,3-dimethyl-6-(aryl)pyrimido[4,5-e]indolizine-2,4(1H,3H)-diones (**4b**, **4c**, **4e**, **4f**, and **4g**) in dichloromethane ($c = 1 \times 10^{-5}$ M) at 20 °C

	4b	4c	4e	4f	4g
$\lambda_{1,\text{abs}}$ (nm)	251	256	264	254	272
$\epsilon_{\lambda_1} \times 10^4$ ($\text{M}^{-1} \text{cm}^{-1}$)	2.1	1.3	2.0	2.1	2.7
$\lambda_{2,\text{abs}}$ (nm)	262	332	327	327	293
$\epsilon_{\lambda_2} \times 10^4$ ($\text{M}^{-1} \text{cm}^{-1}$)	2.0	1.6	0.94	0.97	2.3
$\lambda_{3,\text{abs}}$ (nm)	324		384	375	353
$\epsilon_{\lambda_3} \times 10^4$ ($\text{M}^{-1} \text{cm}^{-1}$)	0.87		0.46	0.42	1.3
$\lambda_{4,\text{abs}}$ (nm)	373				369
$\epsilon_{\lambda_4} \times 10^4$ ($\text{M}^{-1} \text{cm}^{-1}$)	0.37				1.3
$\lambda_{1,\text{em}}$ (nm)	386 ^{a,d}	419 ^a	473 ^a	471 ^a	539 ^b
$\lambda_{2,\text{em}}$ (nm)	469 ^a				
Φ^c	4 ^a	53 ^a	8 ^a	4 ^a	2 ^b

^a Excitation wavelength $\lambda_{\text{ex}} = 330$ nm. ^b Excitation wavelength $\lambda_{\text{ex}} = 370$ nm. ^c Fluorescence standards: quinine hemi-sulphate in H_2SO_4 (0.05 M) ($\Phi = 0.52$). ^d Shoulder.

yields ranging from 2–8%, compound **4c** showed a distinct enhancement of its quantum yield to 53%, which might be explained by the occurrence of certain donor–acceptor relationships between the electron-rich dimethylaniline moiety and the electron deficient uracil ring.

Compound **4g**, representing benzo-indolizinouracil, displayed a red-shifted absorption spectrum, due to the extension of its π -system. The absorption spectrum reveals a certain fine-

structure for **4g**, with a weak, but broad $S_0 \rightarrow S_1$ transition band at 419 nm. Similarly, the emission spectrum is shifted to 539 nm. However, **4g** exhibited the lowest quantum yield among all studied compounds (2%).

Conclusion

In summary, we have developed a novel methodology for the synthesis of indolizinouracils, representing, to the best of our knowledge, a hitherto unknown heterocyclic core structure. The synthetic strategy is based on a chemoselective C–N coupling *via* an addition–elimination reaction of *N,N*-dimethyl-5-bromo-6-chlorouracil with N-heterocycles, followed by Sonogashira cross-coupling reaction with alkynes and InCl_3 -catalysed cycloisomerisation. The obtained products were isolated in moderate to excellent yields under carefully optimised reaction conditions. This methodology is tolerant towards the incorporation of pyrrole and indole as N-heterocyclic entities as well as towards functional groups attached to the aryl ring. Preliminary photophysical properties of selected derivatives have been investigated by steady-state absorption and photoluminescence spectroscopy. The optical properties are strongly altered by the substitution pattern on the indolizinouracil scaffold, with quantum yields ranging from 2 to up to 53%.



Experimental section

General information

Nuclear magnetic resonance spectra ($^1\text{H}/^{13}\text{C}/^{19}\text{F}$ NMR) were recorded on a Bruker AVANCE 300 III, 250II, or 500. The analysed chemical shifts (δ) are referenced to the residual solvent signals of the deuterated solvents, CDCl_3 (δ = 7.26 ppm for ^1H -NMR and 77.16 ppm for ^{13}C -NMR). Multiplicities due to spin–spin correlation are reported as follows: s = singlet, d = doublet, dd = doublet, pt = pseudotriplet, and m = multiplet; they are further described by their coupling constants J . Infrared spectra (IR) were measured as attenuated total reflection (ATR) experiments using a Nicolet 380 FT-IR spectrometer. The signals were characterised by their wavenumbers and the corresponding absorption as very strong (vs), strong (s), medium (m), weak (w) or very weak (vw). UV-vis spectra were recorded on a Cary 60 UV-Vis spectrophotometer, and emission spectra were recorded on an Agilent Cary Eclipse fluorescence spectrophotometer. Basic and high-resolution mass spectra (MS/HRMS) were measured on instruments coupled to a gas chromatograph (GC) or a liquid chromatograph (LC). Samples were ionised by electron impact ionisation (EI) on an Agilent 6890/5973 or Agilent 7890/5977 GC-MS equipped with an HP-5 capillary column using helium carrier gas or by electron spray ionisation (ESI) on an Agilent 1200/6210 Time-of-Flight (TOF) LC-MS. X-ray single-crystal structure analysis was performed on a Bruker Apex Kappa-II CCD diffractometer. The solvent, toluene, was purchased as a dry solvent and used without further purification. Other reagents, catalysts, ligands, acids and bases were used as purchased from commercial suppliers. Column chromatography was performed on Merck Silica gel 60 (particle size 63–200 μm). Solvents for extraction and column chromatography were distilled prior to use.

Representative procedure C for the synthesis of 4a–h

A mixture of **3d** (312 μmol ; 101 mg) and InCl_3 (5 mol%; 327 μmol ; 72.3 mg) was dissolved in dry toluene (2 mL) and stirred for 16 hours under an argon atmosphere at 100 °C. The reaction was monitored by TLC until completion. The reaction was quenched by the addition of saturated NH_4Cl solution (15 mL), the phases were separated, and the aqueous layer was extracted with dichloromethane (3×20 mL). The combined organic layers were dried over Na_2SO_4 , concentrated under reduced pressure and purified by column chromatography (heptane/ethyl acetate).

1,3-Dimethyl-6-(*p*-tolyl)pyrimido[4,5-*e*]indolizine-2,4(1*H*,3*H*)-dione (4a). According to the general procedure C, compound **4a** was obtained as a brown solid in 76% yield (76 mg, 238 μmol , R_f = 0.24 heptane/ethyl acetate, 3 : 2); mp: 203–205 °C. IR (ATR): $\tilde{\nu}$ [cm $^{-1}$] = 1702 (s), 1646 (vs), 1607 (s), 1489 (s), 1450 (s), 1364 (s), 1131 (s), 818 (s). ^1H NMR (300 MHz, chloroform-*d*) δ = 7.7 (dd, J = 3.1, 1.3 Hz, 1H), 7.5–7.4 (m, 2H), 7.2 (s, 1H), 7.2 (d, J = 7.8 Hz, 2H), 6.8 (dd, J = 4.0, 3.1 Hz, 1H), 6.6 (dd, J = 4.0, 1.3 Hz, 1H), 3.8 (s, 3H), 3.4 (s, 3H), 2.3 (s, 3H). ^{13}C { ^1H } NMR (75 MHz, chloroform-*d*) δ = 161.5, 152.7, 139.1, 138.2, 136.5, 134.9, 129.5, 128.7, 128.2,

116.6, 115.0, 113.7, 102.9, 101.0, 37.0, 28.7, 21.4. MS (EI, 70 eV): m/z (%) = 319 (37, M^+), 306 (14), 281 (12), 221 (11), 207 (16), 113 (12). HRMS (EI): calcd for $\text{C}_{19}\text{H}_{17}\text{N}_3\text{O}_2$ [M] $^+$ 319.13153, found: 319.13163.

1,3-Dimethyl-6-phenylpyrimido[4,5-*e*]indolizine-2,4(1*H*,3*H*)-dione (4b). According to the general procedure C, compound **4b** was obtained as a brown solid in 72% yield (72.3 mg, 237 μmol , R_f = 0.34 heptane/ethyl acetate, 3 : 2); mp: 144–146 °C. IR (ATR): $\tilde{\nu}$ [cm $^{-1}$] = 1697 (s), 1640 (vs), 1611 (s), 1479 (s), 1364 (s), 1215 (m), 1195 (m), 756 (s). ^1H NMR (300 MHz, chloroform-*d*) δ = 7.84–7.78 (m, 1H), 7.67–7.61 (m, 2H), 7.51–7.33 (m, 4H), 6.95–6.89 (m, 1H), 6.68 (d, J = 3.8 Hz, 1H), 3.97–3.90 (m, 3H), 3.48 (s, 3H). ^{13}C { ^1H } NMR (75 MHz, chloroform-*d*) δ = 161.5, 152.7, 139.3, 137.8, 136.4, 128.8, 128.7, 128.4, 128.3, 116.7, 115.1, 114.0, 102.9, 101.0, 37.0, 28.8. MS (EI, 70 eV): m/z (%) = 305 (43, M^+), 292 (14), 281 (14), 248 (10). HRMS (EI): calcd for $\text{C}_{18}\text{H}_{15}\text{N}_3\text{O}_2$ [M] $^+$ 305.11588, found: 305.11595.

6-(4-(Dimethylamino)phenyl)-1,3-dimethylpyrimido[4,5-*e*]indolizine-2,4(1*H*,3*H*)-dione (4c). According to the general procedure C, compound **4c** was obtained as a brown solid in 46% yield (46.3 mg, 133 μmol , R_f = 0.20 heptane/ethyl acetate, 3 : 2); mp: 157–159 °C. IR (ATR): $\tilde{\nu}$ [cm $^{-1}$] = 1683 (s), 1650 (vs), 1605 (s), 1514 (s), 1397 (s), 1294 (s), 1205 (s), 1123 (s). ^1H NMR (500 MHz, chloroform-*d*) δ = 7.76 (dd, J = 3.1, 1.3 Hz, 1H), 7.57–7.53 (m, 2H), 7.29 (s, 1H), 6.90 (dd, J = 4.0, 3.1 Hz, 1H), 6.83–6.79 (m, 2H), 6.73 (dd, J = 4.1, 1.3 Hz, 1H), 3.90 (s, 3H), 3.47 (s, 3H), 3.02 (s, 6H). ^{13}C { ^1H } NMR (75 MHz, chloroform-*d*) δ = 161.6, 152.7, 150.5, 138.5, 136.6, 129.1, 128.9, 125.5, 116.4, 114.8, 112.5, 112.4, 102.9, 101.2, 40.6, 37.0, 28.7. MS (EI, 70 eV): m/z (%) = 348 (27, M^+), 333 (15), 207 (12), 149 (6), 123 (8). HRMS (EI): calcd for $\text{C}_{20}\text{H}_{20}\text{N}_4\text{O}_2$ [M] $^+$ 34.15808, found: 348.15744.

6-(4-Fluorophenyl)-1,3-dimethylpyrimido[4,5-*e*]indolizine-2,4(1*H*,3*H*)-dione (4d). According to the general procedure C, compound **4d** was obtained as a brown solid in 86% yield (86.9 mg, 269 μmol , R_f = 0.21 heptane/ethyl acetate, 3 : 2); mp: 217–219 °C. IR (ATR): $\tilde{\nu}$ [cm $^{-1}$] = 1706 (s), 1650 (vs), 1568 (s), 1478 (s), 1357 (s), 1221 (s), 1158 (s), 840 (s). ^1H NMR (300 MHz, chloroform-*d*) δ = 7.82 (dd, J = 3.2, 1.3 Hz, 1H), 7.65–7.56 (m, 2H), 7.31 (s, 1H), 7.20–7.10 (m, 2H), 6.93 (dd, J = 4.0, 3.1 Hz, 1H), 6.62 (dd, J = 4.1, 1.3 Hz, 1H), 3.94 (s, 3H), 3.48 (s, 3H). ^{19}F NMR (282 MHz, chloroform-*d*) δ = -113.6. ^{13}C { ^1H } NMR (75 MHz, chloroform-*d*) δ = 162.8 (d, J = 247.5 Hz), 161.5, 152.7, 139.4, 136.38, 133.8 (d, J = 3.3 Hz), 130.1 (d, J = 8.1 Hz), 127.7, 116.7, 115.8 (d, J = 21.6 Hz), 115.2, 114.1, 102.9, 101.0, 37.1, 28.8. MS (EI, 70 eV): m/z (%) = 323 (100, M^+), 266 (24), 251 (28), 237 (15), 223 (20), 211 (19). HRMS (ESI-TOF): calcd for $\text{C}_{18}\text{H}_{14}\text{FN}_3\text{O}_2$ [M + H] $^+$ 323.10646, found: 323.10613.

1,3-Dimethyl-6-(4-(trifluoromethyl)phenyl)pyrimido[4,5-*e*]indolizine-2,4(1*H*,3*H*)-dione (4e). According to the general procedure C, compound **4e** was obtained as a brown solid in 70% yield (71.8 mg, 192 μmol , R_f = 0.20 heptane/ethyl acetate, 3 : 2); mp: 127–128 °C. IR (ATR): $\tilde{\nu}$ [cm $^{-1}$] = 1704 (s), 1636 (vs), 1609 (s), 1496 (s), 1320 (vs), 1166 (s), 1120 (vs), 1065 (vs). ^1H NMR (300 MHz, chloroform-*d*) δ = 7.84 (dd, J = 3.1, 1.3 Hz, 1H),



7.80–7.69 (m, 6H), 7.38 (s, 1H), 6.95 (dd, J = 4.0, 3.2 Hz, 2H), 6.64 (dd, J = 4.0, 1.3 Hz, 1H), 3.94 (s, 2H), 3.48 (s, 3H). ^{19}F NMR (282 MHz, chloroform-*d*) δ = -62.5. $^{13}\text{C}\{\text{H}\}$ NMR (75 MHz, chloroform-*d*) δ = 161.3, 152.6, 141.4 (d, J = 1.5 Hz), 139.8, 135.9, 130.3 (q, J = 32.6 Hz), 128.7, 127.2, 125.8 (q, J = 3.7 Hz), 124.2 (q, J = 272.1 Hz), 116.9, 115.4, 114.9, 102.8, 100.8, 37.1, 28.8. MS (EI, 70 eV): m/z (%) = 373 (100, M^+), 316 (25), 301 (26), 287 (11), 273 (17). HRMS (EI): calcd for $\text{C}_{19}\text{H}_{14}\text{F}_3\text{N}_3\text{O}_2$ [$\text{M} + \text{H}^+$] 373.10326, found: 373.10309.

1,3-Dimethyl-6-(thiophen-3-yl)pyrimido[4,5-*e*]indolizine-2,4(1H,3H)-dione (4f). According to the general procedure C, compound **4f** was obtained as a brown solid in 78% yield (78.6 mg, 252 μmol , R_f = 0.21 heptane/ethyl acetate, 3 : 2); mp: 200–202 °C. IR (ATR): $\tilde{\nu}$ [cm⁻¹] = 1697 (s), 1645 (vs), 1487 (s), 1475 (s), 1458 (s), 1339 (s), 783 (s), 72 (s). ^1H NMR (300 MHz, chloroform-*d*) δ = 7.78 (dd, J = 3.1, 1.3 Hz, 1H), 7.59 (dd, J = 2.2 Hz, 1H), 7.46–7.42 (m, 2H), 7.41 (s, 1H), 6.93 (dd, J = 4.0, 3.1 Hz, 1H), 6.79 (dd, J = 4.0, 1.3 Hz, 1H), 3.91 (s, 3H), 3.46 (s, 3H). $^{13}\text{C}\{\text{H}\}$ NMR (75 MHz, chloroform-*d*) δ = 161.4, 152.6, 139.1, 138.2, 135.9, 127.6, 126.1, 123.5, 123.0, 116.6, 115.1, 113.6, 102.9, 100.8, 37.1, 28.8. MS (EI, 70 eV): m/z (%) = 311 (100, M^+), 300 (87), 296 (22), 273 (35), 269 (29), 254 (57). HRMS (EI): calcd for $\text{C}_{16}\text{H}_{13}\text{N}_3\text{O}_2$ [M^+] 311.07230, found: 311.07180.

1,3-Dimethyl-6-(*p*-tolyl)pyrimido[5',4':5,6]pyrido[1,2-*a*]indole-2,4(1H,3H)-dione (4g). According to the general procedure C, compound **4g** was obtained as a brown solid in 72% yield (73.3 mg, 198 μmol , R_f = 0.34 heptane/ethyl acetate, 3 : 2); mp: 201–202 °C. IR (ATR): $\tilde{\nu}$ [cm⁻¹] = 1700 (s), 1650 (vs), 1617 (s), 1489 (s), 1446 (vs), 1440 (vs), 1310 (s), 824 (s). ^1H NMR (500 MHz, chloroform-*d*) δ = 7.85–7.81 (m, 1H), 7.76–7.72 (m, 1H), 7.60–7.56 (m, 2H), 7.43–7.39 (m, 2H), 7.36–7.29 (m, 3H), 6.91 (s, 1H), 3.57 (s, 3H), 3.50 (s, 3H), 2.45 (s, 3H). $^{13}\text{C}\{\text{H}\}$ NMR (126 MHz, chloroform-*d*) δ = 161.4, 154.1, 142.5, 139.8, 138.4, 134.5, 132.4, 131.7, 129.6, 129.0, 128.1, 124.3, 121.3, 121.1, 116.9, 115.9, 101.1, 98.1, 39.3, 28.6, 21.4. MS (EI, 70 eV): m/z (%) = 369 (100, M^+), 326 (10), 311 (12), 297 (10). HRMS (EI): calcd for $\text{C}_{23}\text{H}_{19}\text{N}_3\text{O}_2$ [M^+] 369.14718, found: 369.14769.

9-Fluoro-1,3-dimethyl-6-(*p*-tolyl)pyrimido[5',4':5,6]pyrido[1,2-*a*]indole-2,4(1H,3H)-dione (4h). According to the general procedure C, compound **4h** was obtained as a brown solid in 78% yield (79 mg, 204 μmol , R_f = 0.35 heptane/ethyl acetate, 3 : 2); mp: 193–195 °C. IR (ATR): $\tilde{\nu}$ [cm⁻¹] = 1710 (s), 1664 (vs), 1446 (s), 1310 (m), 1141 (s), 1028 (m), 848 (s), 828 (s). ^1H NMR (300 MHz, chloroform-*d*) δ = 7.78 (dd, J = 9.2, 4.3 Hz, 1H), 7.59–7.53 (m, 2H), 7.45 (s, 1H), 7.38–7.29 (m, 3H), 7.08 (td, J = 8.9, 2.6 Hz, 1H), 6.87 (s, 1H), 3.57 (s, 3H), 3.50 (s, 3H), 2.45 (s, 3H). ^{19}F NMR (282 MHz, chloroform-*d*) δ = -117.4. $^{13}\text{C}\{\text{H}\}$ NMR (75 MHz, chloroform-*d*) δ = 161.3, 160.1 (d, J = 242.6 Hz), 154.0, 142.2, 141.2, 138.6, 134.3, 132.7 (d, J = 10.6 Hz), 129.7, 128.8, 128.7, 128.1, 117.6, 117.0 (d, J = 9.9 Hz), 109.7 (d, J = 26.7 Hz), 105.8 (d, J = 23.6 Hz), 101.4, 97.9 (d, J = 4.7 Hz), 39.2, 28.6, 21.4 (signals of two carbons are absent, which may relate to signal overlap). MS (EI, 70 eV): m/z (%) = 387 (100, M^+), 372 (13), 344 (11), 35 (18), 301 (9), 271 (6). HRMS (ESI-TOF): calcd for $\text{C}_{23}\text{H}_{19}\text{FN}_3\text{O}_2$ [$\text{M} + \text{H}^+$] 388.1461, found: 388.1462.

Data availability

All data that support the findings of this study are available in the published article and/or the ESI† of this article.

Conflicts of interest

There are no conflicts or financial interest to declare.

Acknowledgements

We are grateful for the financial support provided by the State of Mecklenburg-Western Pomerania (Germany) and for the technical and analytical support from the University of Rostock (Germany) and Leibniz Institute for Catalysis (Germany).

References

- 1 L. M. de Coen, T. S. A. Heugebaert, D. García and C. V. Stevens, *Chem. Rev.*, 2016, **116**, 80–139.
- 2 M. S. Mohamed, S. A. Ali, D. H. A. Abdelaziz and S. S. Fathallah, *BioMed Res. Int.*, 2014, **2014**, 249780.
- 3 (a) V. O. Iaroshenko, M. Vilches-Herrera, A. Gevorgyan, S. Mkrtchyan, K. Arakelyan, D. Ostrovskyi, M. S. Abbasi, L. Supe, A. Hakobyan, A. Villinger, D. M. Volochnyuk and A. Tolmachev, *Tetrahedron*, 2013, **69**, 1217–1228; (b) M. M. Hammouda, K. M. Elattar, A. Y. El-Khateeb, S. E. Hamed and A. M. A. Osman, *Mol. Diversity*, 2024, **28**, 927–964; (c) P. Seboletswe, P. Awolade and P. Singh, *ChemMedChem*, 2021, **16**, 2050–2067.
- 4 J. F. Campos, T. Besson and S. Berteina-Raboin, *Pharmaceuticals*, 2022, **15**, 352.
- 5 F. Buron, J. Y. Mérour, M. Akssira, G. Guillaumet and S. Routier, *Eur. J. Med. Chem.*, 2015, **95**, 76–95.
- 6 (a) L. Baziyan, P. Ahmadi, S. Zare Gheshlaghi, M. Behrouz, M. Emami, M. Saeedi, A. Ebrahimi, L. Emami and S. Khabnadideh, *J. Mol. Struct.*, 2024, **1302**, 137435; (b) S. Pathania and R. K. Rawal, *Eur. J. Med. Chem.*, 2018, **157**, 503–526.
- 7 (a) J. I. Bardagí and R. A. Rossi, *Org. Prep. Proced. Int.*, 2009, **41**, 479–514; (b) W. Zhao-Li, L. An-Di, L. Li and C. Liang, *Synlett*, 2024, 603–615; (c) F. Kopp and P. Knochel, *Org. Lett.*, 2007, **9**, 1639–1641; (d) N. Boudet and P. Knochel, *Org. Lett.*, 2006, **8**, 3737–3740; (e) A. Pałasz, *Monatsh. Chem.*, 2008, **139**, 1397–1404.
- 8 R. M. F. de Abreu, T. Brockmann, A. Villinger, P. Ehlers and P. Langer, *Beilstein J. Org. Chem.*, 2024, **20**, 898–911.
- 9 R. M. F. de Abreu, P. Ehlers and P. Langer, *Beilstein J. Org. Chem.*, 2024, **20**, 2708–2719.
- 10 (a) J. Campanini-Salinas, J. Andrades-Lagos, G. Gonzalez Rocha, D. Choquesillo-Lazarte, S. Bollo Dragnic, M. Faúndez, P. Alarcón, F. Silva, R. Vidal, E. Salas-Huenuleo, M. Kogan, J. Mella, G. Recabarren Gajardo and



D. Vásquez-Velásquez, *Molecules*, 2018, **23**, 1776; (b) B. A. Lanman, J. R. Allen, J. G. Allen, A. K. Amegadzie, K. S. Ashton, S. K. Booker, J. J. Chen, N. Chen, M. J. Frohn, G. Goodman, D. J. Kopecky, L. Liu, P. Lopez, J. D. Low, V. Ma, A. E. Minatti, T. T. Nguyen, N. Nishimura, A. J. Pickrell, A. B. Reed, Y. Shin, A. C. Siegmund, N. A. Tamayo, C. M. Tegley, M. C. Walton, H.-L. Wang, R. P. Wurz, M. Xue, K. C. Yang, P. Achanta, M. D. Bartberger, J. Canon, L. S. Hollis, J. D. McCarter, C. Mohr, K. Rex, A. Y. Saiki, T. San Miguel, L. P. Volak, K. H. Wang, D. A. Whittington, S. G. Zech, J. R. Lipford and V. J. Cee, *J. Med. Chem.*, 2020, **63**, 52–65; (c) M. N. Nasr and M. M. Gineinah, *Arch. Pharm.*, 2002, **335**, 289; (d) Y. Shen, Q. Xie, Y. Wang, J. Liang, C. Jiang, X. Liu, Y. Wang and C. Hu, *Bioorg. Chem.*, 2023, **141**, 106848.

11 T. Inazumi, K. Yamada, Y. Kuroki, A. Kakehi and M. Noguchi, *J. Chem. Soc., Perkin Trans. 1*, 1994, 557–564.

12 [Der Titel “Gantasala, Fournet *et al.* 2023 – Accessing spiro-piperidines from dihydropyridones” kann nicht dargestellt werden. Die Vorlage “Literaturverzeichnis - Zeitschriftenaufsatz - (Standardvorlage)” beinhaltet nur Felder, welche bei diesem Titel leer sind.].

13 W. Pfleiderer and H. Deiss, *Isr. J. Chem.*, 1968, **6**, 603–614.

14 A. Fürstner and V. Mamane, *J. Org. Chem.*, 2002, **67**, 6264–6267.

15 B. Martín-Matute, C. Nevado, D. J. Cárdenas and A. M. Echavarren, *J. Am. Chem. Soc.*, 2003, **125**, 5757–5766.

16 (a) W. Yang, R. R. Kazemi, N. Karunathilake, V. J. Catalano, M. A. Alpuche-Aviles and W. A. Chalifoux, *Org. Chem. Front.*, 2018, **5**, 2288–2295; (b) A. Fürstner, V. Mamane, G. Seidel and D. Laurich, *Org. Synth.*, 2006, **83**, 103–110.

17 S. R. Meech and D. Phillips, *J. Photochem.*, 1983, **23**, 193–217.

